Direct radiative capture calculations on ^{56}Fe

Georgios Gkatis[1,2,*], *Maria* Diakaki[2], *Alberto* Mengoni[3,4,5], and *Gilles* Noguere[1]

[1]CEA/DES/IRESNE/DER/SPRC/LEPh, Cadarache, F-13108 Saint Paul Lez Durance, France
[2]Department of Physics, National Techical University of Athens (NTUA), GR-15780 Athens, Greece
[3]European Organization for Nuclear Research (CERN), CH-1211 Geneva, Switzerland
[4]Istituto Nazionale di Fisica Nucleare (INFN), IT-40127 Sezione di Bologna, Italy
[5]Agenzia nazionale per le nuove tecnologie (ENEA), IT-00196 Roma, Italy

Abstract. The theoretical description of the ^{56}Fe neutron induced reaction cross sections is the subject of many studies within the nuclear data community. Based on these studies, issues were discovered in the evaluated cross sections of the ^{56}Fe(n,γ) reaction. Those issues were addressed by implementing changes in the ENDF/B-VIII.0 evaluation. The aim of this work is to provide a physical interpretation for these changes by exploring the direct radiative capture mechanism for ^{56}Fe. For the calculations, a dedicated code (PDIX) was utilized. The first results of the direct capture cross section of ^{56}Fe are presented and discussed.

1 Introduction

Iron is used in various applications within the nuclear industry, primarily due to its favorable mechanical and thermal properties. As a structural material, iron and its alloys are widely employed in the construction of nuclear reactors and other nuclear facilities. Due to their strength, durability, and good heat transfer properties, iron-based materials are suitable for the construction of pressure vessels, steam generators, piping systems, and other structural components inside a nuclear power plant. Additionally, these materials are used in the design of casks and containers for the storage and transportation of spent nuclear fuel. These containers provide structural integrity and radiation shielding to ensure the safe handling and storage of radioactive materials. For the above reasons, accurate neutron cross section data of iron are crucial for optimizing reactor performance, ensuring safe and efficient operation, and developing effective shielding systems that reduce radiation exposure.

The neutron cross section data of iron were extensively studied under the Collaborative International Evaluated Library Organization (CIELO) project [1]. In the case of the ^{56}Fe(n,γ) reaction cross section, major changes were made within the project, and the results were adopted by the ENDF/B-VIII.0 evaluation [2]. The background from 700 to 850 keV was readjusted to reproduce the experiments performed at RPI [3]. In this measurement, a "bump" in the capture yield was observed at around 850 keV. The increase of the (n,γ) cross section in this region cannot be described via the R-Matrix theory. Also, it is interesting to mention that in this energy the inelastic scattering channel opens, so one would expect the capture cross section to decrease and not the opposite.

*e-mail: georgios.gkatis@cea.fr

Furthermore, a background cross section component was added in the energy range from 10 eV to 100 keV. The enhancement of the capture cross section in this region was based on the criticality benchmark HEU-MET-INTER-001 (ZPR-9/34). It was observed that when the ENDF/B-VII.1 evaluation [4] was used, the benchmark's eigenvalue was overestimated by more than 1000 pcm. It was realized that by making a minor readjustment in this energy region, it became possible to bring the HEU-MET-INTER-001 result within the experimental uncertainty, while minimally impacting other benchmarks. As seen in Fig.1a the added background cross section demonstrates a nearly 1/v behavior.

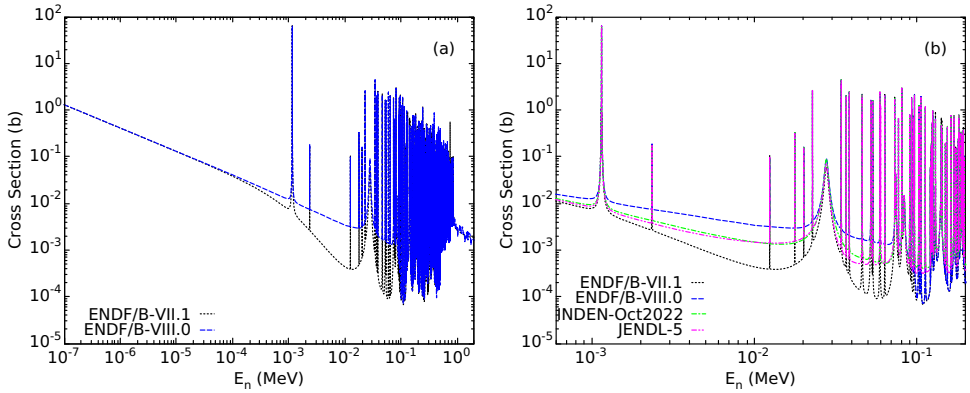

Figure 1: (a) Evaluated ^{56}Fe(n,γ) cross section of ENDF/B-VII.1 [4] (black) and ENDF/B-VIII.0 [2] (blue) from thermal up to 2 MeV neutron energy. (b) Comparison of the ^{56}Fe(n,γ) evaluated cross section of ENDF/B-VII.1 [4] (black), ENDF/B-VIII.0 [2] (blue), INDEN-Oct2022 [5] (green), and JENDL-5 [6] (magenta) in the 10 eV - 100 keV region.

The cross-section data of iron are currently under study by the International Nuclear Data Evaluation Network (INDEN) [5], coordinated by the International Atomic Energy Agency (IAEA). In the latest evaluation released by INDEN in October 2022, the background component in the 10 eV - 100 keV region was reduced by more than 50% of what was introduced in the ENDF/B-VIII.0 evaluation (Fig. 1b). This intermediate choice for the background component was still able to reproduce the HEU-MET-INTER-001 benchmark, and it also proved to be optimal for the ASPIS/Fe-88 benchmark. This change was also supported by the latest JENDL evaluation, JENDL-5 [6], where direct and semi-direct calculations for ^{56}Fe have been included.

In the present work, an effort to provide a physical interpretation of these changes is attempted by exploring the direct radiative capture on ^{56}Fe.

2 Direct radiative capture calculations

The theoretical concept behind direct radiative capture is described in detail in [7–9]. In principle, two capture mechanisms exist. First is the *compound capture*, where the incident neutron is captured and a long-lived compound system is formed. This compound nucleus is typically in an excited state due to the addition of the neutron and it de-excites by releasing excess energy in the form of one or more gamma rays. Second is the *direct capture*, where the incident neutron is captured by the target without any compound state formation. Direct capture occurs by exciting a limited number of degrees of freedom within a shorter time frame, which reflects to the duration it takes for the projectile to traverse the target.

The compound capture cross section can be theoretically described using several formalisms. Statistical methods, such as the Hauser-Fesbach formalism, is used to calculate the probability of the gamma-ray emission and predict the cross section based on the statistical properties of the compound nucleus. Furthermore, the R-Matrix formalism is used to describe the presence of nuclear resonance peaks, where the cross section exhibits sharp energy-dependent variations. On the other side, the theoretical model that is used to calculate the direct capture component considers the specific quantum mechanical properties of the neutron-target system. It takes into account the spatial distribution of the nucleons within the target nucleus, their orbital angular momenta, and the properties of the neutron-nucleus potential. The direct capture capture cross section is proportional to the single-level electromagnetic transition matrix element. For the emission of an electric dipole radiation (E1) from the initial to final state, and for a specific neutron incident energy E_n, it is given by:

$$\sigma_{n,\gamma} = \frac{16\pi}{9\hbar} k_\gamma^3 \bar{e}^2 |Q_{i\to f}^{(E1)}|, \tag{1}$$

where $k_\gamma = \epsilon_\gamma/\hbar c$ is the wave number of the emitted γ-ray with energy ϵ_γ, and $\bar{e} = -Z/A$ is the E1 effective charge of the neutron [8, 10]. Based on Eq. (1), the cross section is primarily estimated by the matrix element:

$$Q_{i\to f}^{(E1)} = < \Psi_i | \hat{T}^{E1} | \Psi_f > \equiv \sqrt{S_f} \cdot I_{i,f} \cdot A_{i,f}, \tag{2}$$

where $\hat{T}^{E1} = rY^{(E1)}(\theta, \phi)$ is the dipole operator, Ψ_i represents the wave function of the initial state, and Ψ_f the wave function of the final state. The matrix element can be expressed as the multiplication of three terms, in which $I_{i,f}$ is the radial part of the transition matrix elements, $A_{i,f}$ is the angular coupling part, and S_f is the spectroscopic factor of each bound state which can be determined experimentally.

The dedicated code (PDIX) used in the present work was developed by A. Mengoni. It performs the calculation in two steps. First, the bound state wave functions are determined based on available experimental data, and then the direct capture cross section is calculated for a given optical model potential (OMP). For the calculation of the bound state wave functions, 107 levels are available in ENSDF [11] for ^{57}Fe. The evaluation is based on experimental data obtained by three different reactions, namely ^{56}Fe(d,p), ^{57}Fe(p,p'), and ^{59}Co(d,a) [12–14]. In the present study, a grouped version of all the levels was used based on the work of H. M. Sen Gupta [13] (Table 1). Calculations were performed using either the 107 individual states available in ENSDF or the 6 group-states proposed by H. M. Sen Gupta. It was observed that both calculations provide similar results.

Table 1: List of the bound states of ^{57}Fe that were used in this work along with their corresponding energy and spectroscopic factor.

States	Averaged values	
	Energy (MeV)	Spectroscopic factor (S_f)
$2p_{\frac{3}{2}}$	1.02	0.78
$2p_{\frac{1}{2}}$	2.97	1.26
$1f_{\frac{5}{2}}$	2.06	0.97
$1g_{\frac{9}{2}}$	4.03	0.61
$2d_{\frac{5}{2}}$	4.77	0.67
$3s_{\frac{1}{2}}$	5.06	0.11

Once the wave functions of the bound states have been calculated, the direct capture cross section can be determined for a specific optical model potential. In principle the phenomenological optical model potential for nucleon-nucleus scattering is defined as

$$U(r,E) = -V_V(r,E) - iW_V(r,E) - iW_D(r,E) + iW_{SO}(r,E).\mathbf{l}.\sigma + V_{SO}(r,E).\mathbf{l}.\sigma + V_C(r), \quad (3)$$

where V_C is the Coulomb term, $V_{V,SO}$ is the real part and $W_{V,D,SO}$ is the imaginary part of the volume-central (V), surface-central (D), and spin-orbit (SO) potentials [15]. In the case of direct neutron capture, since their is no formation of a compound system, the imaginary part of the OMP is set to zero, and also the Coulomb potential is null because the projectile is not a charged particle. The remaining volume-central potential was described as a Woods-Saxon potential of the type

$$V_V(r) = \frac{-V_0}{1 + exp[(r-R)/a]}. \quad (4)$$

In the present work, several calculations where performed, testing different OMP parameters in order to study the effect in the final outcome. In the end, the OMP parameters proposed by A. J. Koning for the case of ^{56}Fe were used as the optimal choice [15]: a well depth of $V_0 = 53$ MeV, radius of $r_0 = 1.244$ fm, diffuseness of $a = 0.603$ fm, and a spin-orbit coupling potential with strength $V_{SO} = 6$ MeV.

3 Preliminary results

In Fig. 2 the preliminary results of the calculations are presented along with the ENDF/B-VII.1 and ENDF/B-VIII.0 evaluations, from thermal up to 2 MeV neutron incident energy.

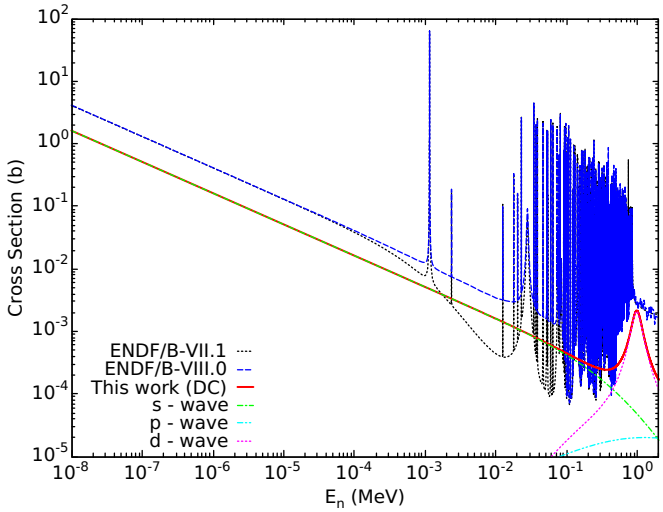

Figure 2: The results of the direct radiative capture cross section of ^{56}Fe (red) compared with the ENDF/B-VII.1 (black) [4] and ENDF/B-VIII.0 (blue) [2] evaluations from thermal up to 2 MeV neutron energy. The partial contributions of the s-wave (green), p-wave (cyan), and d-wave (magenta) direct capture are also presented with dash-lines.

Based on these relusts it is noticed that the *s-wave* direct capture is able to partially reproduce the 1/v background in the 10 eV - 100 keV energy region that was added in the

ENDF/B-VIII.0 evaluation. Additionally, the *d-wave* direct capture looks like a good candidate to reproduce the "bump" in the cross section around 850 keV that was observed in the measurement performed at RPI. It needs to be clarified that in this calculation no interference effect between direct and compound capture was taken into account.

3.1 Comparison with TALYS

The nuclear code TALYS [16] is also able to calculate the direct capture cross section. The direct capture formalism that was implemented in the code is described in detail in [17]. TALYS has the capability to calculate both the direct and the semi-direct cross section for all transitions. Since the calculations performed in this work were focused only on the direct capture cross section for E1 transitions, a comparison with TALYS was made in order to asses the effect of the semi-direct and the other transitions to the final result. To be consistent, the default OMP parameters of TALYS were used in both calculations. In Fig. 3 the resulting direct capture cross section of TALYS and of the code used in this study are presented. The

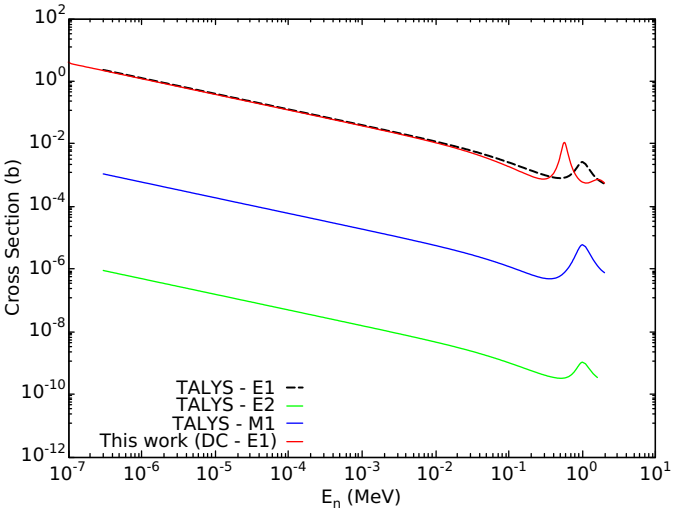

Figure 3: Comparison of the direct capture cross section of ^{56}Fe for an E1 transition between the TALYS code (black) and the code used in the present work (red). The cross sections of TALYS for E2 (green) and M1 (blue) transitions are also presented.

outcome of both codes illustrates that the E1 transitions are the main contributors to the direct capture cross section, since the TALYS cross sections for the E2 and M1 transitions are negligible. By comparing the results of both codes, it is obvious that the semi-direct part has a little or no impact on the final cross section until ~0.5 MeV, since the 1/v s-wave component is the same in magnitude in both cases, and only a small difference in the d-wave "bump" of the cross section is observed, that might be caused by variations in the formalisms used in the two codes.

3.2 Calculation of the total capture cross section in the RRR

In order to calculate the total capture cross section with PDIX, the direct radiative capture formalism was coupled to a Single-Level Breit-Wigner resonance model [18]. For the present

calculations the resonance parameters provided by the JEFF-3.1.1 evaluation were used [19]. In this evaluation, a total of 317 resonances are available, going as high as 850 keV neutron incident energy. To simultaneously reproduce the coherent scattering length and the cross section at thermal energy the Γ_γ parameter of the -2.44 keV resonance was reduced by almost 50%. At the same time, the OMP parameters for the direct capture component where slightly modified in order to properly reproduce the cross section at thermal energy. The depth of the volume potential was reduced by 0.5 MeV compared to the value that was proposed by A. J. Koning.

The code used in this work is able to calculate the total capture cross section at 0 K. To be able to properly compare the result with the evaluated data the Doppler broadening effect needs to be taken into account. To address that, the resulting cross section was folded with the Maxweel-Boltzman distribution

$$\bar{\sigma}(E) \approx \frac{1}{\Delta_D \sqrt{\pi}} \int_{-\infty}^{\infty} dE' e^{\left(-\frac{E'-E}{\Delta_D}\right)^2} \sqrt{\frac{E'}{E}} \sigma(E'), \tag{5}$$

where Δ_D is the Doppler width defined as $\Delta_D = \sqrt{\frac{4Ek_BT}{M/m_n}}$ [20]. The cross section was then calculated for room temperature at 293 K. In Fig. 4 the first results of the total capture cross section are presented.

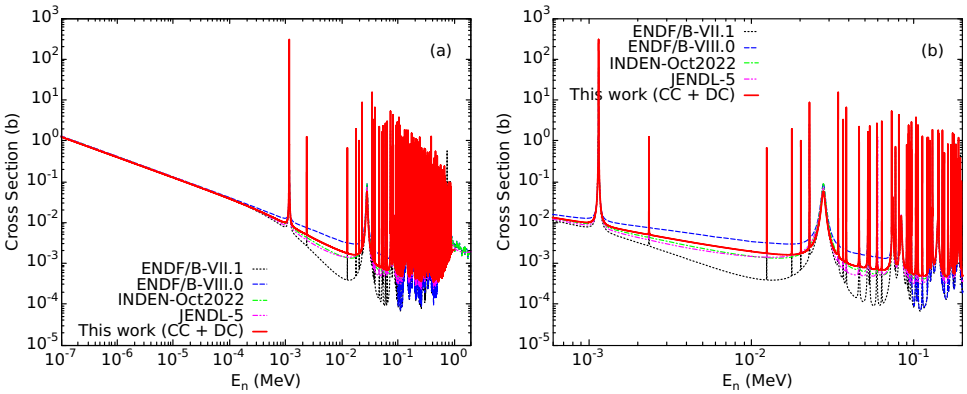

Figure 4: (a) The result of the total capture cross section (red) from thermal up to 2 MeV neutron energy compared to the evaluated ^{56}Fe(n,γ) cross section of ENDF/B-VII.1 (black) [4], ENDF/B-VIII.0 (blue), INDEN-Oct2022 (green) [5], and JENDL-5 (magenta) [6]. (b) The same result in the 10 eV - 100 keV region.

Results of this work support the intermediate choice of the background cross section component that was added in the 10 eV - 100 keV energy region. Even though there are some small differences in this region between this work, INDEN-Oct2022, and JENDL-5 the trend of the cross section is the same in all cases. It is interesting to mention that the present results are very close to the JENDL-5 evaluation, considering that in this evaluation direct and semi-direct calculations have been included. Additionally, in the resolved resonance region from 100 to 850 keV the direct capture component is able to reproduce the background cross section that was added up to 500 keV neutron incident energy and partially cover the rest from 500 to 850 keV, where adjustments were made in order to reproduce the RPI experiment.

4 Conclusions

The direct radiative capture mechanism for the case of ^{56}Fe was explored in this work. A short description of the steps needed to calculate the direct capture cross section is given and the first results are presented in this contribution. Overall, the s-wave direct capture is able to explain the background component that was added in the 10 eV - 100 keV energy region, while the d-wave direct capture seems to be a good candidate for the "bump" of the capture cross section around 850 keV that was observed at a recent experiment. Finally, a first attempt to calculate the total capture cross section (direct and compound capture) was made using the Single-Level Breit-Wigner formalism to describe the resolved resonance region. The preliminary results of this attempt are very close to the most recent evaluation data for the ^{56}Fe(n,γ) cross section provided by INDEN and JENDL. Fine tuning the resonance parameters is still needed, in order to reduce the small discrepancies between the outcome of this work and the evaluated files.

References

[1] M. Herman et al., Nuclear Data Sheets **148**, 214-253 (2018)
[2] D. A. Brown et al., Nuclear Data Sheets **148**, 1-142 (2018)
[3] B. McDermott et al., EPJ Web of Conferences **146**, 11038 (2017)
[4] M. B. Chadwick et al., Nuclear Data Sheets **112**, 2887-2996 (2011)
[5] INDEN at https://www-nds.iaea.org/INDEN/
[6] O. Iwamoto et al., Journal of Nuclear Science and Technology **60**, 1-60 (2023)
[7] A. M. Lane et al., Nuclear Physics **17**, 563-585 (1960)
[8] A. Mengoni et al., Physical Review C **52**, R2334 (1995)
[9] J. E. Lynn, *The theory of neutron resonance reactions* (Clarendon, Oxford, 1968)
[10] T. Kikuchi et al., Physical Review C **57**, 2724 (1998)
[11] ENSDF at https://www.nndc.bnl.gov/ensdf/
[12] A. Sperduto et al., Physical Review **134**, B142 (1964)
[13] H. M. Sen Gupta et al., Nuclear Physics A **160**, 529-549 (1971)
[14] J. H. Bjerregaard et al., Nuclear Physics **51**, 641-666 (1964)
[15] A. J. Koning et al., Nuclear Physics A **713**, 231-310 (2003)
[16] A. J. Koning, EDP Sciences, 211-214 (2008)
[17] Yi Xu et al., Physical Review C **86**, 045801 (2012)
[18] Y. Nagai et al., Physical Review C **102**, 044616 (2020)
[19] A. Santamarina et al., JEFF Report **22**, NEA/OECD (2009)
[20] F. H. Frohner, JEFF Report **18**, NEA/OECD (2000)